

139 THE STRUCTURE OF CONVECTIVE SYSTEMS OBSERVED BY PHASED ARRAY RADAR IN THE KINKI REGION, JAPAN

Sho Yoshida¹, Tomoo Ushio², Satoru Yoshida²,
Shigeharu Shimamura², Kouichi Maruo², Nozomu Takada¹

¹*Meteorological Engineering Center, Inc.*

²*Graduate School of Engineering, Osaka University*

1. INTRODUCTION

Localized and short-term heavy rainfall generated by convective systems often cause disasters in Japan. In particular, urban flash floods, which have short response time of less than an hour, threaten the safety of urban residents. To mitigate the effects of such disasters, real time observation and accurate short-term forecasting (nowcasting) of rainfall is required.

National Research Institute for Earth Science and Disaster Prevention (NIED) installed X-band (wave length is near 3 cm) multiparameter (XMP) radars around the Tokyo metropolitan area for the real monitoring of severe weather. Kato and Maki (2009) showed that XMP radar is more useful to detect localized heavy rainfall than currently operational radars (C-band) installed by Japan Meteorological Agency. Additionally, Kato et al. (2010) and Yoshida et al. (2012) used XMP radar data as initial data for nowcasting to improve accuracy of initial data set. However, temporal resolution is not enough

to investigate the temporal development of thunderstorms (Kim et al. 2012). Also, high spatial resolution data in the upper level is effective to forecast evolution of thunderstorms (Hirano and Maki, 2010, Nakakita et al. 2012).

To solve these problems, Osaka University developed the phased array radar (PAR) at X band in Japan. PAR can scan very rapidly (30 seconds for full volume scan) with the high resolution of azimuthal 1.2 degrees and range 0.1 km. PAR is expected to apply to analyze temporal change of thunderstorms.

We used the phased array radar data to investigate convective systems which cause local and short-term heavy rainfall, mainly from the viewpoints of their vertical structure and process of development.

2. DATA

2.1 Phased array radar

In this study, we used the phased array radar (PAR) at X-band developed by Osaka University, located at 34.82°N 135.52°E in Kinki region (red square in Fig. 1). The volume scan interval of the phased array radar was 30 seconds with 120 elevations from 0.5 to 90 degrees. Data was obtained up to 60 km from the radar site with 100 m range resolution and 1.2 degrees beam width. To analyze the structure of convective systems,

* *Corresponding author address:*

Sho Yoshida, Meteorological Engineering Center, Inc., Kyomachibori, Nishi-ku, Osaka, 550-0003, Japan.
E-mail: s.yoshida@meci.jp.

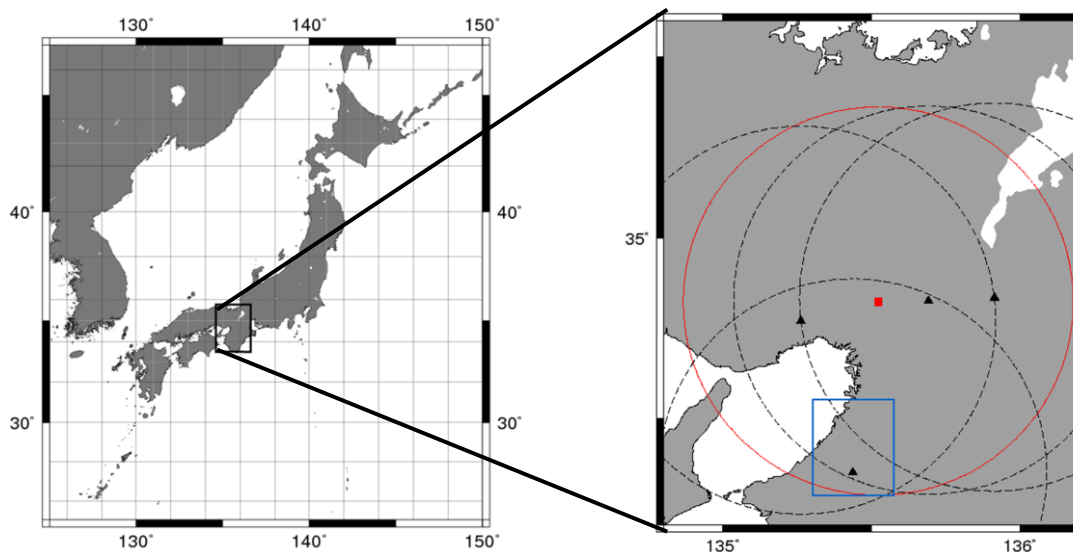


Fig.1. Location and observation area of radars. Red square and circle indicate PAR site at Osaka University and observation area, respectively. Black triangles and broken circles indicate XMP radar sites and observation area, respectively. Blue square indicates analysis target domain.

this data was interpolated into Cartesian coordinates with 0.1 km horizontal and vertical resolutions through weighting function (Cressman, 1959).

2.2 XMP radar

The Ministry of Land, Infrastructure, Transport and Tourism (MLIT) installed X-band multiparameter (XMP) radars network around main cities in Japan to monitor severe weather. In the Kinki region, four XMP radars were installed (black triangles in Fig. 1). These XMP radars can scan constant altitude data (almost 1 km height) every 1 minute with only parameter of rainfall rate, and full volume data every 5 minutes with polarimetric parameters. We also used XMP radar data to compare to the PAR.

3. RESULTS

3.1 Definition of targets

In this study, a convective cell (CC), a convective system (CS) and a reflectivity core (RC) are defined as follows. Convective cell (CC) is the region where reflectivity is more than 30 dBZ and a single peak exists at 1km height (If there are two peaks, divided into two convective cells). Convective system (CS) is the region which is composed of single or multiple convective cells. Reflectivity core (RC) is the region where reflectivity is more than 45 dBZ in each convective cell.

3.2 Case overview

Localized heavy rainfall was caused by convective systems at the domain about 40 km south from Osaka University (PAR site) on 1

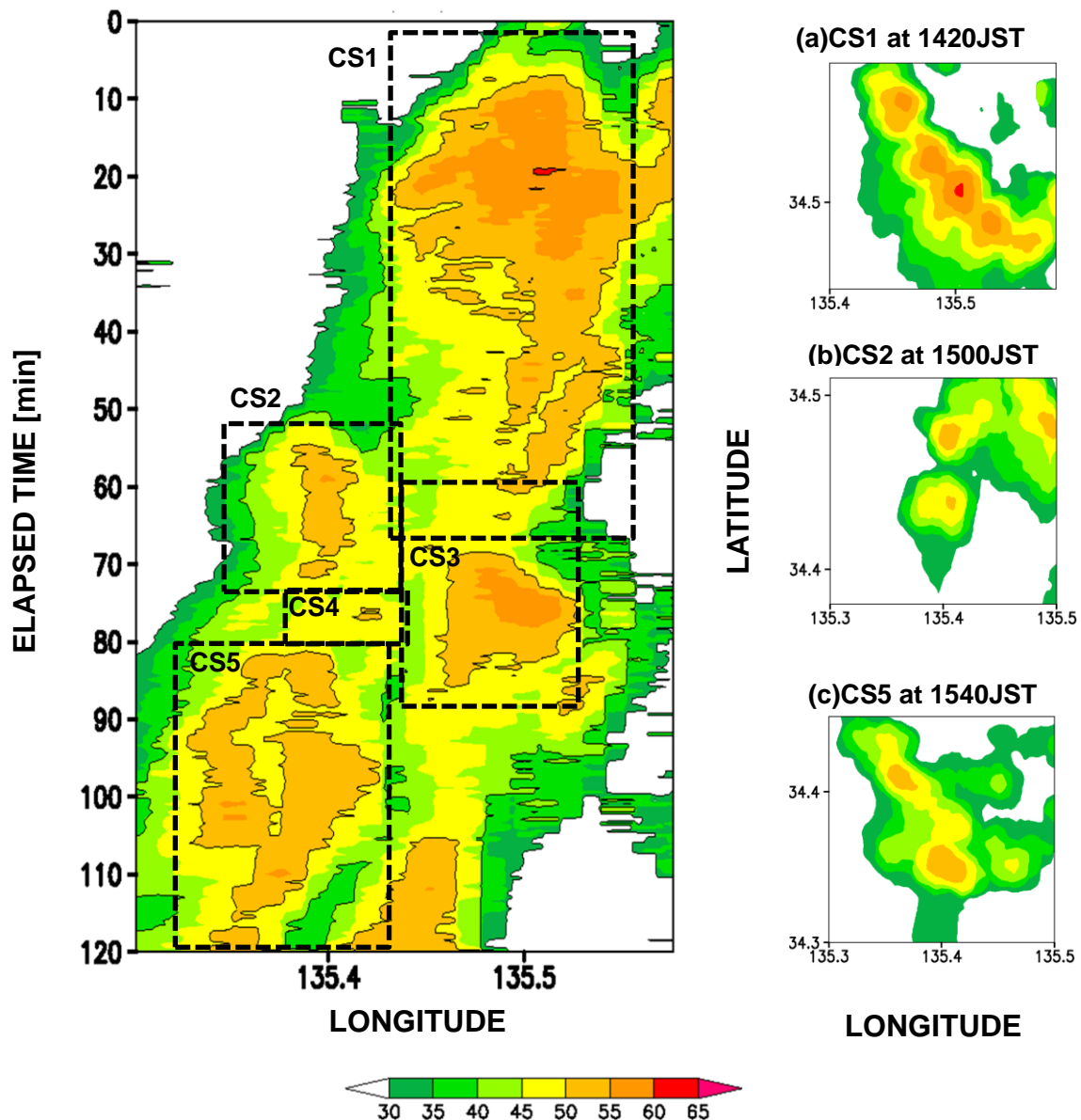


Fig. 2 Hovmoller diagram of maximum reflectivity at 1 km height (left panel) and snapshot of CS1, CS2 and CS4 at 1420(a), 1500(b), 1540(c) JST, respectively. Vertical axis of hovmoller diagram indicates elapsed time from 1400 JST.

September 2012 (blue rectangle in Fig. 1). Figure 2 shows hovmoller diagram of maximum reflectivity obtained by PAR at 1 km height. Five clear convective systems (CS1 to CS5 in Fig. 2) are identified between 1400 to 1600 JST. The first convective system (CS1) was formed

around 1400 JST. Around this time, some small scale convective cells were generated and these convective cells merged each other around 1413 JST, and moved very slowly to northwest. On the other hand, the second convective system (CS2) was formed at the south of CS1 around 1450

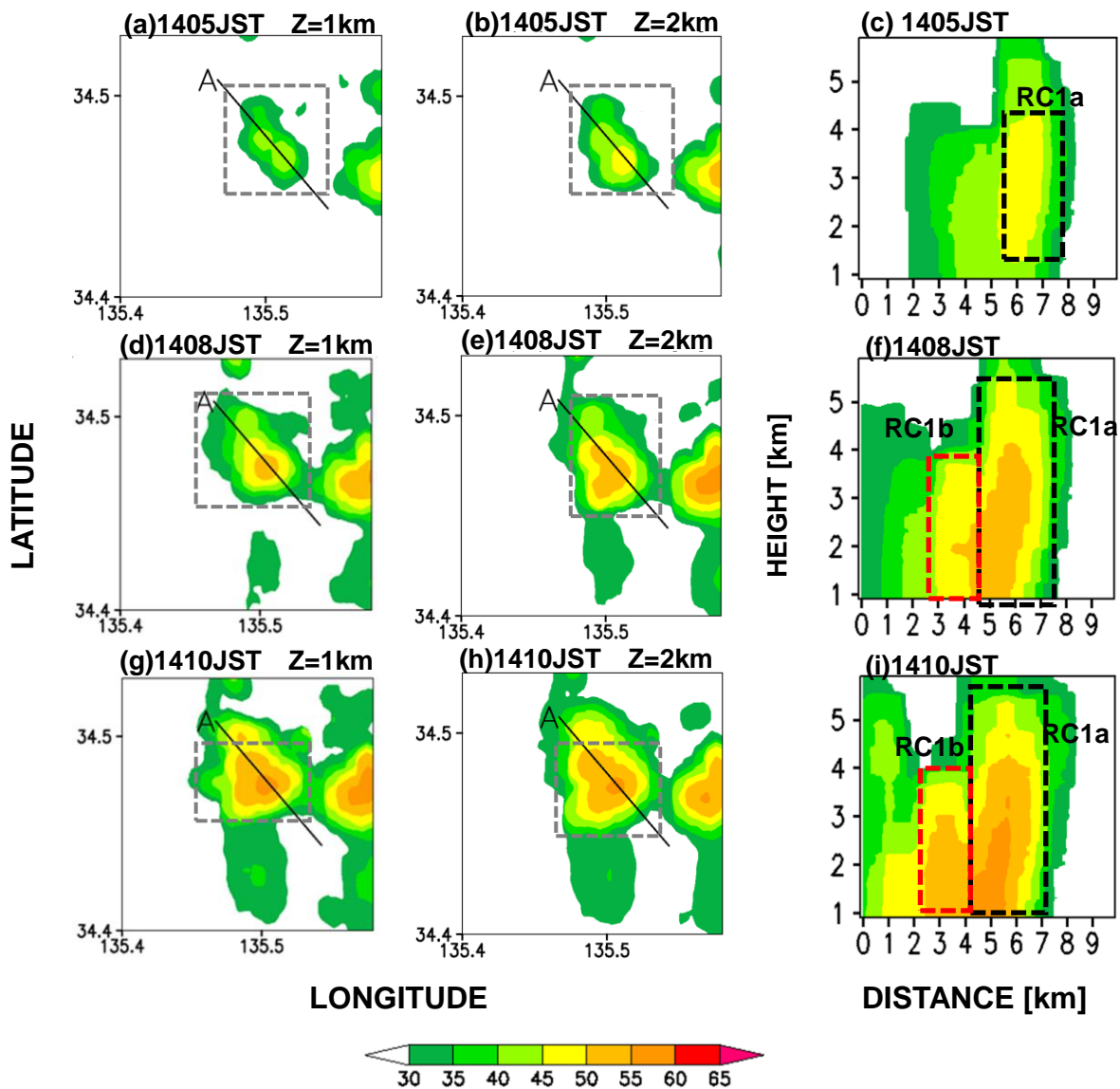


Fig. 3 Horizontal distribution of reflectivity at 1 km height (a, d and g) and at 2 km height (b, e and h), and vertical cross section of reflectivity along line A at 1405(c), 1408(f) and 1410(i) JST.

JST. This convective system was also organized with some small scale convective cells, and moved to north. At 1505 JST, CS1 and CS2 were merged and moved to west very slowly. The third and fourth convective systems (CS3 and CS4) were organized at 1500 and 1515 JST, respectively. Finally, all of the convective systems were merged at 1530 JST (CS5).

3.3 Vertical structures of convective system

To investigate the temporal development of convective cells, the vertical cross section of CS1 from 1405 to 1410 JST is shown in Fig. 3.

The relatively weak convective system which had two weak reflectivity peaks less than 45 dBZ (gray dotted rectangle) at 1 km height was

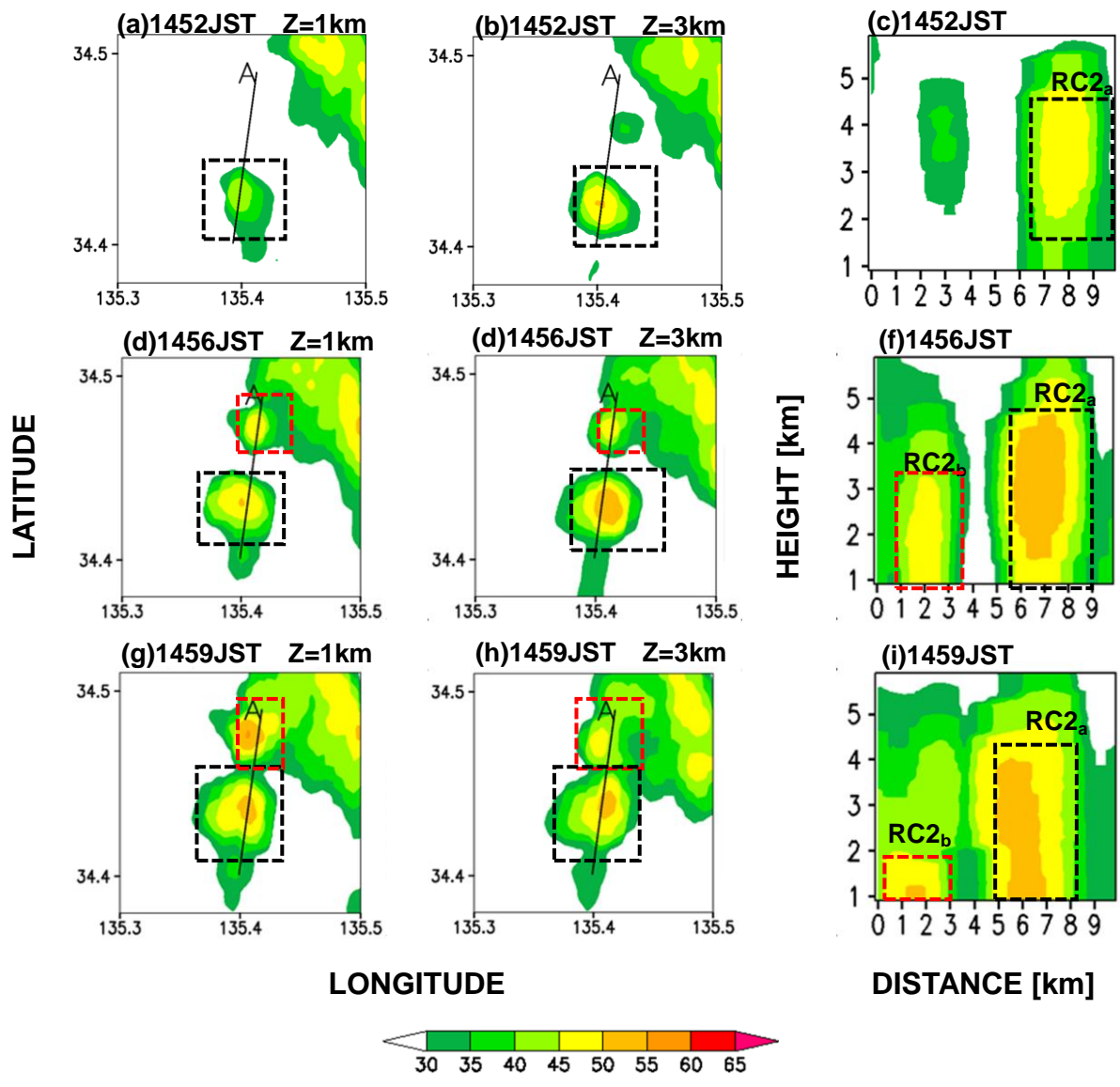


Fig. 4 Same as Fig. 3, but for case CS2.

observed at 1405 JST. This convective system developed and then its maximum reflectivity exceeded 55 dBZ at 1410 JST. On the other hand, radar echo whose peak reflectivity was more than 45 dBZ was observed at 2 km height. The echo was stronger than one at 1 km height. According to the vertical cross section, the echo top of this convective cells reached to 6 km

height and the relatively core (RC1a) was located at about 2 km height at 1405 JST. At this time, RC1a had not reach 1 km height. RC1a was gaining reflectivity as descending to the ground. Furthermore, new reflectivity core which had a weak reflectivity relative to RC1a was observed along line A at 1408 JST (RC1b). At 1410 JST, a seed of another reflectivity core

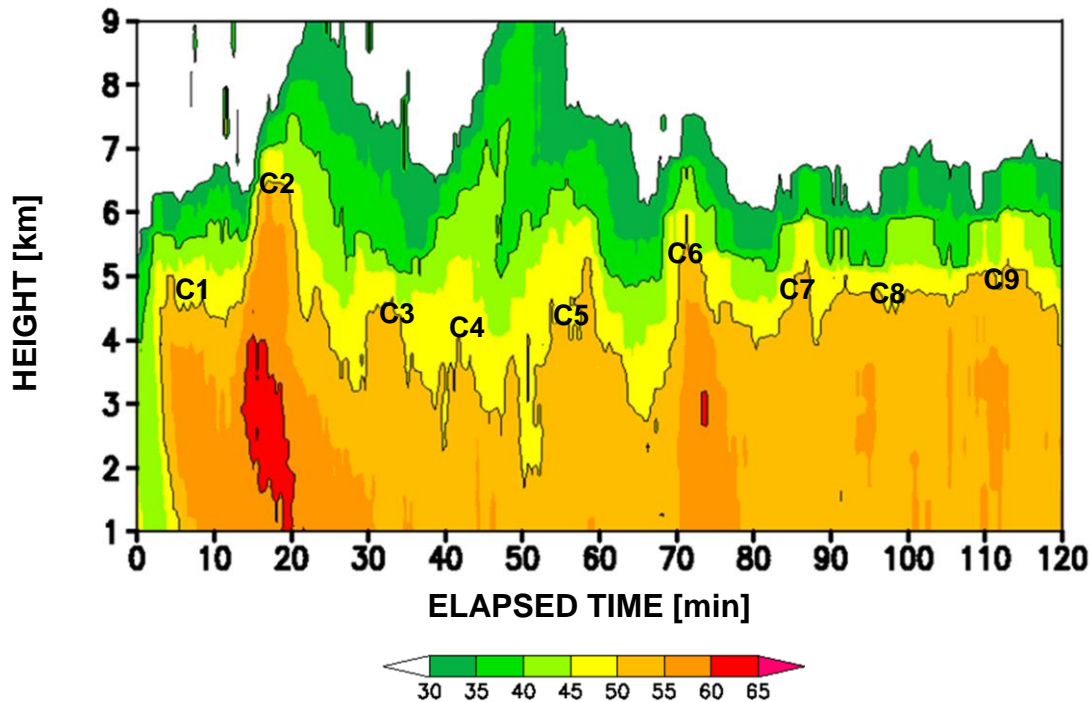


Fig. 5 Time-height cross section of maximum reflectivity of target domain shown in Fig.1. Horizontal axis indicates elapsed time from 1400 JST.

which had a weak reflectivity peak was also observed at 4 km height around 1 km distance. Such reflectivity core generation cycle lasted, and then a linear convective system was formed at 1420 JST (See Fig.2a).

Horizontal distribution and vertical cross section of CS2 from 1452 to 1459 JST is shown in Fig. 4. As same as CS1, convective cell (black dotted rectangle) with reflectivity less than 45 dBZ was observed at 1 km height at 1452 JST and this cell developed as it moved very slowly to north. At 1459 JST, a peak reflectivity of this cell reached more than 50 dBZ. Also, another convective cell was observed at north side of RC2a at 1km height at 1456 JST (red dotted rectangle) and this convective cell had reflectivity more than 55 dBZ at 1459 JST. These

temporal evolutions were identified at upper level in previous time step. In the vertical cross section along line A, two reflectivity peaks were observed around 4 km height at 1452 JST. These peaks developed at upper level and descended to the ground.

The temporal change in the vertical profiles of maximum reflectivity of target domain is shown in Fig.5. At least nine reflectivity cores can be identified from 1400 to 1600 JST (C1-C9).

These cores recurred every 10 minutes and formed at 3 to 5 km height. This height is quite general for convective precipitation cores in Japan.

4. DISCUSSION

Hirano and Maki (2010) discussed the

availability of the vertically integrated liquid (VIL) water content product from XMP radar in NIED (5 minutes interval), focusing on a localized severe rainfall. In this discussion, VIL values from XMP radar were well consistent with gauge measurements. Furthermore detection by VIL had a lead time of 5–10 minutes than gauge measurements. Also, Kim et al. (2012) suggested the availability of volume scan data with VIL, however they also suggested that more fine temporal resolution data was needed to detect temporal evolution of precipitation cells.

In this study, PAR detected the detailed time changes of reflectivity cores. As the result, it was found that these reflectivity cores reached ground a few minutes after they had generated at upper level. On the other hand XMP radars failed to detect some of the temporal evolution and detailed structure of reflectivity cores, because XMP radar needs 5 minutes to scan full volume data while PAR can scan it in 30 seconds. The comparison demonstrates an advantage of PAR over conventional methods in terms of detection of temporal evolution.

5. CONCLUSIONS

We used PAR data to investigate life cycle and vertical structure of convective systems which caused localized heavy rainfall at the point about 40 km south from Osaka University (PAR site) on 1 September 2012

The convective cells which organized convective systems were generated and dissipated repeatedly. These temporal changes can be identified with reflectivity at upper level in

advance. Reflectivity cores were formed around 5 km height and descended to the ground in about 10 minutes. On the other hand, XMP failed to detect these temporal changes, because the temporal resolution of full volume data was not sufficient. The comparison demonstrates the advantage of PAR over conventional methods in terms of detection of temporal evolution.

Furthermore, detection of the reflectivity core in real time is prospective to be new indexes for more accurate short time forecasting.

REFERENCES

- Cressman, G. P., 1959: An operational objective analysis system. *Mon. Wea. Rev.*, **87**, 367–374.
- Hirano K., and M. Maki, 2010: Method of VIL calculation for X-band polarimetric radar and potential of VIL for nowcasting of localized severe rainfall –case study of the Zoshigaya downpour, 5 August 2008-. *SOLA*, **6**, 89-92.
- Kato A., and M. Maki, 2008: Localized heavy rainfall near Zoshigaya, Tokyo, Japan on 5 August 2008 observed by X-band polarimetric radar -Preliminary analysis-, *SOLA*, **5**, 89-92
- _____, M. Maki, K. Iwanami, 2009: Nowcasting of precipitation based on complementary application of X-band polarimetric radar and C-band conventional radar, *Journal of Japan Society of Hydrology and Water Resources*, **22**, 372-385
- Kim D.-S., M. Maki and D.-I. Lee, 2012: X-band dual-polarization radar observations of

precipitation core development and structure in a multi-cellular storm over Zoshigaya, Japan, on August 5, 2008, *J. Meteor. Soc. Japan*, **90**, 701-719.

Nakakita E., R. Nishiwaki, Y., Watanabe and K. Yamaguchi, 2013: Research on the prognostic risk of baby cell for guerilla-heavy rainfall considering by vorticity with doppler velocity, *J. JSCE*, Ser.B1, **69**, 325-330(in Japanese)

Yoshida S., R. Misumi, S. Shimizu, T. Maesaka, K. Iwanami and M. Maki, 2012: Validation of short-term forecasting of meso- γ -scale convective systems based on a cell-tracking system, *SOLA*, **8**, 141-144.